International Journal of Computer Information Systems and Industrial Management Applications
ISSN 2150-7988 Volume 18(8s) 2026 pp. 19-35
https://doi.org/10.70917/ijcisim-2026-3216
Article

Proximity Coupling and Defected Ground Structure for Enhanced 2x1 MIMO Microstrip Patch Antenna Performance in UWB Applications

Amol C. Bhosale[1], Nagashettappa M. Biradar[2], Sujeet More[3]

[1] Department of Electronics and Communication Engineering, RV Institute of Technology and Management (RVITM), VTU, Bengaluru, Karnataka, India.
Email: amol5210@gmail.com
ORCID: 0000-0002-5088-1964
[2] Department of Electronics and Communication Engineering, RV Institute of Technology and Management (RVITM), VTU, Bengaluru, Karnataka, India.
Email: nagashettappab.rvitm@rvei.edu.in
ORCID: 0000-0002-8760-5517
[3] Department of Computer Engineering, Trinity College of Engineering and Research, Pune, Maharashtra, India.
Email: sujeetmore7@gmail.com
ORCID: 0000-0002-6107-122X

Abstract: This research paper introduces an innovative method aimed at improving the performance of a 2x1 MIMO circular microstrip patch antenna (MPA) precisely designed for Ultra-Wideband (UWB) requests. The investigation utilizes the Proximity Coupling feeding technique alongside a Defected Ground Structure (DGS) to enhance critical performance indicators such as bandwidth, gain, and signal reliability. The antenna, with dimensions of 25x15 mm, shows notable progress in reducing mutual coupling and increasing isolation among the antenna elements, which are essential for efficient MIMO functionality. The incorporation of DGS is demonstrated to optimize the electromagnetic characteristics of the antenna's ground plane, further boosting its performance by minimizing unwanted radiation modes and improving impedance matching. Detailed simulations performed using High-Frequency Structure Simulator (HFSS) software indicate that the proposed MIMO antenna achieves a reoccurrence loss of -15.9 dB, a gain of 2.417 dB, and a directivity of 4.35 dB at a resonant frequency of 4.83 GHz, with a Diversity Gain surpassing 10.00 dB. These findings highlight the efficacy of the proposed design in addressing the growing requirements for high data rates and enhanced signal quality in contemporary wireless communication systems. The results contribute to the ongoing advancement of antenna technology, providing valued perceptions for future research and progress in this domain.
Keywords: Multiple input multiple output (MIMO), Ultra-Wideband (UWB), Defected ground structure (DGS), Proximity Coupling feeding, Microstrip Patch and ECC.

1. Introduction

In the contemporary landscape, advancements in wireless communication technology are occurring at a remarkable pace. Various cellular communication systems are being developed to enhance their speed, reliability, and energy efficiency. As these technologies evolve, the role of antenna devices becomes increasingly critical in optimizing the performance of cellular networks. In environments characterized by multipath propagation, MIMO (Multiple Input Multiple Output) expertise serves as an active remedy for multipath fading, utilizing multiple antennas at both the transmitter and receiver ends. To mitigate fading in open space, MIMO employs signalling practices such as spatial multiplexing and space-time coding. Consequently, the integration of Ultra-Wideband (UWB) technology with MIMO is essential for modern wireless communication systems.

The microstrip patch antenna stands out as one of the most suitable antennas for RF applications and wireless systems, primarily due to its affordability and compact size. Its small dimensions, low production costs, lightweight, and ease of integration with other components have made microstrip antennas particularly appealing for wireless mobile communication and satellite applications. However, a notable drawback of the microstrip patch antenna is its limited bandwidth. Various strategies exist to augment the bandwidth of these antennas, through a typical microstrip patch antenna achieving a gain of around 6 dB. Techniques to increase bandwidth include modifying the patch geometry and adjusting higher-order modes.

Recently, ultra-wideband (UWB) technology has gained traction among researchers and academics, attributed to its extensive bandwidth, high data transmission capabilities, and commercial viability within a lower power density spectrum. Over the past decade, UWB technology has experienced rapid growth, thanks to its advantageous characteristics, including higher data rates at reduced power consumption. The UWB spectrum operates within an unrestrained frequency range of 3.1 to 10.6 GHz.

- ❖ The key contributions of this study are outlined below:
- ❖ - MIMO technology is employed to enhance the transmission and reception capabilities of multiple streams by augmenting the circular microstrip patch.
- ❖ - The integration of DGS represents a notable advancement in antenna performance, influencing the electromagnetic fields surrounding the antenna.
- ❖ - The proximity coupling feeding method is utilized to optimize the interaction of radiating components, resulting in higher data rates and enhanced signal reliability.
- ❖ - The combination of the Proximity Coupling feeding technique with DGS leads to a substantial enhancement in the recital of the MIMO circular microstrip cover antenna.

2. Literature review

In 2019, Biswas, A.K., and Chakraborty, U. [16] introduced an antenna design featuring an electromagnetic band gap (EBG) edifice aimed at reducing mutual coupling among its ports. The experimental investigation utilized a line feed method for activation. This antenna achieved a fractional bandwidth of 64%, operating in the frequency assortment of 2 to 3.9 GHz. The proposed MIMO antenna demonstrated significant diversity gain along with a remarkably low envelope correlation coefficient.

In 2018, Zhang, Z., and colleagues [17] presented a study that introduced two innovative designs of defected ground structures (DGS) to mitigate mutual coupling and minimize cross-polarization in MIMO antennas. The research developed unique periodic fractal DGSs (PFDGSs), which effectively reduced mutual coupling by 20 dB. Additionally, a second arc-shaped DGS was implemented beneath each patch to further decrease the level of cross-polarization.

In 2019, Hasan, M.N., and his team [18] proposed a monopole antenna featuring a defective ground design, incorporating two strategically placed slits and a notch to enhance impedance bandwidth. To optimize impedance matching, a U-shaped stub was added to the radiator. The measured impedance bandwidth of the projected monopole antenna spanned from 3 to 11 GHz.

In 2020, Shiddanagouda, F.B., et al. [19] introduced a quad-port MIMO antenna featuring a microstrip line feed and utilizing flawed ground structures. This MIMO antenna effectively covered the 4.1 GHz and 5.9 GHz frequency bands for wireless requests. The design achieved mutual coupling among the elements with isolation levels exceeding -33 dB and -25 dB in the respective bands, attributed to the defected octagon split-ring slot (OSRSDGS) and various rectangular edge slits on the metal surface. In 2019, Nguyen, N.L. [20] showcased a DGS-based MIMO antenna comprising two sets of 2 x 2 elements, centered around a core frequency of 5.3 GHz. The integration of a DGS on the ground plane facilitated low mutual coupling while maintaining high gain. The array demonstrated impressive isolation exceeding 20 dB between its elements and achieved a radiation efficiency of 93%, creation it suitable for a wide array of practical requests due to its manufacturability and efficiency.

In 2021, Khan, M.K., et al. [21] developed a compact two-port MIMO antenna designed for ultra-wideband (UWB) requests. The antenna was constructed through two symmetrical radiators on an FR4 substrate, measuring 34 x 18 x 1.6 mm^3. It exhibited excellent impedance matching across the UWB spectrum and was powered by a 50-ohm microstrip line. To mitigate mutual coupling between the radiating elements, a T-shaped stub was incorporated into the design. In 2017, The author in [22] proposed a compact MIMO UWB antenna with high isolation. This design, consisting of two UWB slot antennas, was notably smaller than traditional UWB antennas with a single element, measuring just 22 x 26 mm². The T-shaped slot remained etched into the surface to enhance low-frequency impedance matching and minimize mutual coupling at frequencies of 4 GHz and above.

In 2021, Tang, X., et al. [23] introduced a binary high-performance UWB MIMO antenna utilizing DGS, U-shaped branches, and stepped impedance stubs. The calculated impedance bandwidth ranged from 2.57 to 12.2 GHz, achieving a remarkable 131%. The S12 parameter for this antenna reached a peak measured value of -15 dB within the impedance bandwidth. Notably, except for the 9-10 GHz range, the method resulted in a channel capacity loss of fewer than 0.4 bit/s/Hz across the entire bandwidth. In 2014, Islam, M.S., et al. [24] presented a microstrip patch antenna (MPA) designed with DGS for narrowband applications, which operated on a single ISM band channel. The antenna exhibited a return loss of approximately -30 dB and resonated at a frequency of 2.45 GHz, achieving a high gain of 7.04 dBi. The practice of a faulty ground structure enhanced the antenna's efficiency, resulting in a 17.63% increase in realized gain.

In the same year, Nawale, P.A., and Zope, R.G. [25] tackled challenges associated with Rectangular Microstrip Patch Antennas (RMPA) by introducing various problematic configurations to the ground plane. Their approach of employing a defective ground plane significantly improved the bandwidth of patch antennas, which had been a major limitation. They successfully expanded the antenna's bandwidth by 34.1846 MHz, making it suitable for wideband applications. The antenna was simulated at 2.4 GHz using CAD-FEKO software.

Sohi, A.K., and Kaur, A. [26] developed a dual-port aperture-coupled Microstrip Antenna (MSA) selection featuring a circular fractal design for extraordinary data rate UWB-MIMO communication systems, utilizing VPM. The proposed array measured 34 x 68.7 x 3.245 mm³ and was constructed on two layers of FR-4 substrate. The ground's aperture slots were transformed into complementary quadrilateral spirals and a tree-shaped DGS, facilitating the desired operational band of 4.6 to 16.8 GHz.

In 2021, Sohi, A.K. and colleagues [27] presented a modeled and tested three-band-stop aperture-coupled two-port adapted Pythagorean tree fractal antenna designed for ultra-wideband uses. The proposed array was constructed using two FR-4 substrates measuring 37.5 x 81.5 mm², featuring a feed network on the lower substrate and two enhanced Pythagorean tree fractal radiators on the upper substrate. The ground-etched apertures were transformed into a hexagonal spiral configuration, which enhanced the multiband response of the fractal geometry across a wide operational bandwidth.

In 2020, Jamal, M.Y. and team [28] introduced a planar, compact, and polarization-diverse MIMO (Multiple-Input, Multiple-Output) patch antenna. To ensure instantaneous matching and isolation among the two patches through offset feeding for circular polarization, they incorporated three grounded stubs along with a mirrored F-shaped defective ground structure. The antenna components were densely arranged at the targeted frequency of 2.5 GHz, with an edge-to-edge spacing of just 0.06 mm.

In 2019, Babu, K.V. and associates [29] showcased a multi-band circular MIMO radiator, both with and without a parasitic element shaped like a dumbbell, aimed at wireless applications. The proposed antenna featured a U-shaped inverted slot, two rectangular slits, and a circular MIMO radiating patch. The replicated outcomes indicated that the multi-band antenna could cover a adequate bandwidth for entire frequency bands, as the far-field values were assessed over a broad operational bandwidth. The circular design radiator maintained consistent and satisfactory radiation patterns, regardless of the presence of the dumbbell-shaped parasitic element.

In the same year, the author in [30] identified besides reported a flaw in the ground plane of a compact monopole ultra-wideband (UWB) antenna. By adding four arcs to each corner of the square patch, they successfully developed a UWB antenna that operates within the frequency range of 3.1 to 10 GHz. They enhanced spatial diversity by positioning the antenna fundamentals closely together while minimizing strong mutual coupling.

The performance of a MIMO 2x1 circular microstrip patch antenna tailored for UWB applications is significantly improved through the innovative technique presented in this study. This approach leverages the Proximity Coupling feeding mechanism along with the Defected Ground Structure (DGS). The Proximity Coupling technique has revolutionized antenna design by enhancing performance through the utilization of electromagnetic interactions among the radiating components. By meticulously designing the feeding network, which encompasses the arrangement of feed lines and the positioning of coupled elements, this method ensures that the radiating elements operate cohesively, leading to enhanced gain, bandwidth, and radiation efficacy. The suggested MIMO 2x1 circular microstrip patch antenna is intended to transmit and receive signals across the entire UWB spectrum with high reliability. Furthermore, the introduction of the DGS is a crucial aspect of our methodology. The DGS effectively mitigates surface waves, refines radiation patterns, and boosts overall antenna performance, making it a vital element in contemporary microstrip antenna designs. By integrating a thoughtfully designed DGS into our MIMO antenna system, we reduce the adverse effects of surface waves and unwanted radiation, resulting in more efficient and clearer transmission and reception of UWB signals.

2.1 Defected Ground Structure

Defected ground structure (DGS) enhances system performance by deliberately adapting the ground plane metal in microstrip, strip line, or coplanar waveguide circuits. This structure stands formed by etching a specific outline, referred to as a "defect," from the ground plane. The various shapes and sizes of these defects disrupt the current distribution within the ground plane, leading to the measured excitation and propagation of electromagnetic waves concluded the substrate. This alteration also influences the capacitance and inductance of a transmission line. Essentially, any irregularity etched into the ground plane of a microstrip can result in an increase in effective capacitance besides inductance. To optimize performance, the defect's design can be transformed from a simple form to a more intricate one. Numerous DGS configurations have been recognized, including hexagonal, cross, rectangular, circular, square, dumbbell, spiral, L-shaped, concentric ring, U-shaped, and V-shaped, along with interdigital DGS. Figures 1 (a) to (e) illustrate various DGS shapes, such as dumbbell, spiral, H, U, and arrowhead designs.

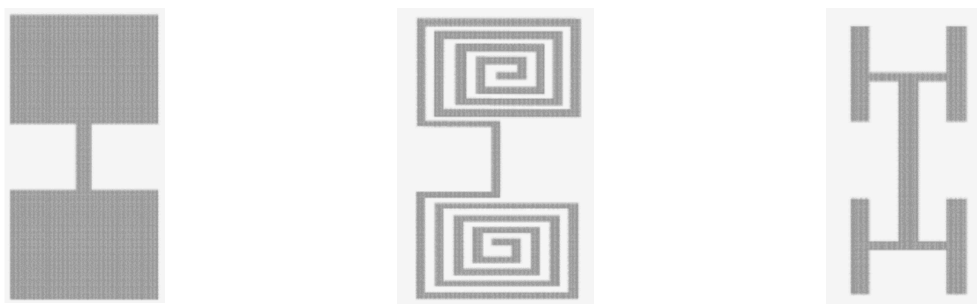

(a). Dumbbell shaped (b). Spiral shaped (c). H- shaped

(d). U- shaped (e) . Arrow head shaped

Figure 1. Various shapes of DGS

Periodic Defected Ground Structures (DGS) are characterized by the regular repetition of unit cells, which leads to enhanced performance and more profound attributes. In transmission lines featuring periodic designs, low-pass filters exhibit defined pass and rejection bands. Key features of these periodic structures include an increased slow-wave effect and additional equivalent components, both of which can be leveraged to minimize circuit dimensions. The term "periodic" pertains to the repetitive nature of physical structures. The depth and bandwidth of the stop-band in a DGS circuit are likely influenced by the number of periods created through the cascading of DGS resonant cells within the ground plane. Among various designs, the H-shaped DGS has been selected for the proposed antenna due to its versatility and effectiveness across different applications, making it a favored option in the design of microstrip antennas and microwave circuits.

2.2 MIMO microstrip antenna geometry and design

The patch antenna features a circular radiating element printed on the primary substrate. This proposed antenna measures 25 mm in distance, 15 mm in width, and has a thickness of 3.2 mm. It exhibits an input impedance of 50Ω. The microstrip feed line is positioned on the higher side of the secondary substrate, which also includes a ground plane and two H-shaped DGS slots on its lower side. The antenna is fed using a proximity-coupled feed, situated 1.6 mm above the bottom substrate. Figure 2 illustrates the MIMO circular patch antenna.

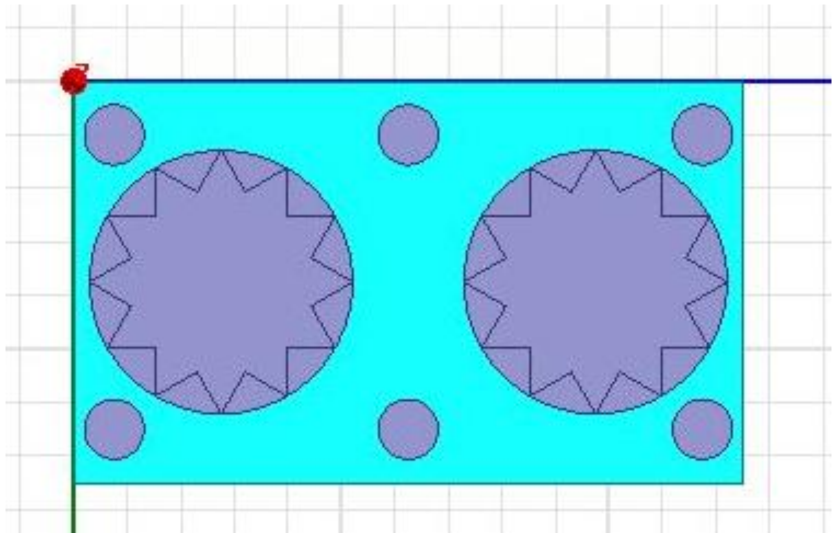

Figure 2. Proposed MIMO circular patch

The radiation elements constitute the primary component in the design of MIMO antennas. In this context, Microstrip Patch Antennas (MPAs) are utilized as the radiation elements. The proposed antenna structure features two circular rings functioning as microstrip patches. The assortment of a dielectric substrate is a crucial first step. Losses are categorized into three types: dielectric loss, conductor loss, and radiation loss. Utilizing a thicker substrate can lead to increased radiation losses and exacerbate the detrimental effects of surface waves. Conversely, reducing the substrate height enhances the suppression of the upper mode and minimizes radiation leakage.

A modified circular ring patch, featuring a radius of 4.92 mm and incorporating three segmented polygons within the circle, has been introduced to attain the desired configuration. Additionally, six parasitic elements, each a small circle with a radius of 1.11 mm, are fabricated on an FR4 substrate. This substrate has a dielectric constant of 4.4, a height of 1.6 mm, and a dielectric loss tangent of 0.02. The design equation, which facilitates the calculation of the proposed antenna's dimensions, is derived from numerical equations within the transmission model. Subsequently, the width of the patch elements is established. Variations in this width will influence the directivity factor, radiation resistance, and other characteristics of the microstrip antenna. These parameters significantly affect the antenna's frequency bandwidth and radiation efficiency. Therefore, the selection of width is crucial for optimizing the frequency range to accomplish the best balance amongst bandwidth and radiation efficiency. The following equation is utilized to calculate the width of the patch.

$$w = \frac{c}{2f_r}\sqrt{\frac{2}{\varepsilon_r}} \quad (1)$$

where c = light's speed in free space, ε_r= relative dielectric constant, and f_r = resonance frequency. It results in acceptable dimensions and good radiation efficiencies. It is necessary to consider an effective dielectric constant that approximates the value given by to account for the fringing effect.

$$\varepsilon_{reff} = \frac{\varepsilon_r+1}{2} \quad (2)$$

The formula for the effective patch length is

$$L_{eff} = \frac{c}{2f_r\sqrt{\varepsilon_{reff}}} \quad (3)$$

The patch length extension ΔL is provided by

$$\Delta L = \frac{0.412\,(\epsilon_{reff}+0.3)\,(\frac{W}{h}+0.264)}{(\epsilon_{reff}-0.258)\,(\frac{W}{h}+0.8)} \quad (4)$$

The precise patch length is provided by L.

$$L = L_{eff} - 2\Delta L \quad (5)$$

The proposed proximity coupling feed for the antenna enhances the performance of MIMO antennas. This feeding method is commonly known as the electromagnetic coupling scheme. In this configuration, the radiating patch is positioned atop the upper substrate, with the feed line located between the two dielectric substrates. A key benefit of this feeding technique is its ability to eliminate unwanted feed radiation while simultaneously achieving a significantly high bandwidth, attributed to the increased total area of the MPA. Figure 3 illustrates the DGS model.

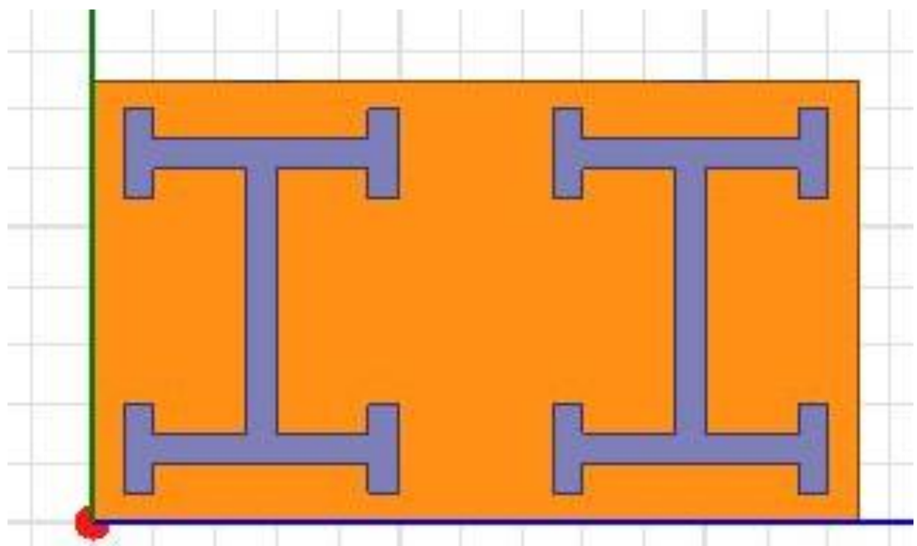

Figure 3. Simulated DGS model

2.3 Proposed MIMO antenna with DGS

To minimize the coupling between microstrip antenna unit cells, an H-shaped Defected Ground Structure (DGS) was designed, etched onto the ground plane, and positioned beneath the two circular radiation patches. This DGS enhances the effective capacitance and inductance of the transmission line. According to transmission line theory, certain imperfections in the etched ground plane disrupt the flow of shielded currents on the same plane, leading to variations in the capacitances and inductances of the transmission lines. On the same substrate, two microstrip antenna elements are arranged in an H-shape, with the ground plane situated on the opposite side. This configuration effectively diminishes the coupling amongst the antenna elements. A simple rectangular slot connects the two H-shaped DGSs vertically, and this unit DGS consists of three basic components, each measuring 3 mm. Figure 4 illustrates the DGS-shaped unit.

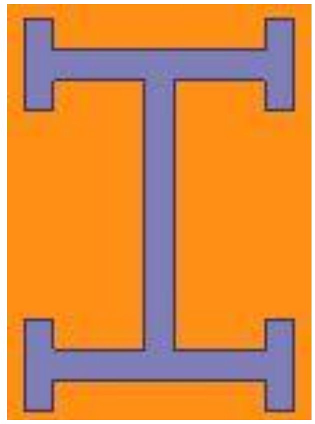

Figure 4. Single H shaped DGS model

3. Outcomes and Discussion

The recital of the proposed antenna is assessed concluded various criteria. Its performance characteristics are analyzed using the High Frequency Structure Simulator (HFSS) software, specifically Version 15.0. HFSS is recognized as the industry standard for simulating three-dimensional full-wave electromagnetic fields and operates on a Linux platform based on Debian. The software provides results for the electric and magnetic fields, current, S-parameters, and both near besides far field radiation patterns. The effectiveness of HFSS as an engineering design tool relies on its automated solution methodology, which allows users to simply input geometry, material specifications, and desired outcomes. This tool facilitates the automatic generation of a suitable, effectual, and accurate mesh to solve the problem at hand. The proposed MIMO antenna is analyzed and compared in configurations both with and without DGS. Key limitations of the proposed MIMO antenna include return loss, gain, directivity, isolation, Envelope Correlation Coefficient (ECC), and Diversity Gain (DG).

3.1 Antenna Parameters

The effectiveness of a MIMO microstrip antenna is often assessed by examining a variety of factors. These factors encompass antenna gain, return loss, directivity, wrapper correlation coefficient (ECC), besides diversity gain (DG).

(i) Antenna Gain

Antenna gain quantifies the enhancement of power density popular a specific direction relative to an isotropic radiator. This measurement is usually represented in decibels relative to isotropic (dBi). A higher antenna gain signifies a more focused radiation pattern.

$$G = \frac{4\pi . U\ (\theta,\varphi)}{P_{in}} \qquad (6)$$

Where the intensity of a given direction is denoted as $U\ (\theta, \varphi)$ and the input power is the P_{in}.

(ii) Directivity

The term used to describe the relative strength of a radiation's power in a specific direction compared to its overall power is known as directivity. This parameter assesses antenna's capability to emphasis the emitted vitality in a designated direction. A higher directivity signifies a more concentrated radiation pattern.

$$D = \frac{4\pi\ U}{P_{rad}} \qquad (7)$$

Where U is the radiation intensity and P_{rad} is the radiation power.

(iii) Radiation pattern

The radiation design of an antenna characterizes its radiation characteristics in relation to its orientation, either through mathematical equations or graphical illustrations.

(iv) Return loss

Return loss quantifies the amount of influence that an antenna reflects back into a transmission line. This measurement is determined by the ratio of incident power to reflected power. A higher return loss designates improved impedance matching and a reduction in signal loss.

$$RL = -20\log_{10}\left[\frac{VSWR-1}{VSWR+1}\right] \tag{8}$$

(v) Isolation

In a multi-antenna system, isolation refers to the power that is coupled between adjacent radiating patches. Isolation is quantified using S-parameters, specifically the S12 and S21 parameters, which are relevant in the context of a two-element MIMO antenna.

(vi) ECC

The correlation coefficient indicates the extent to which two communication channels are related. The ECC illustrates the correlation among the individual antenna elements. It is advisable to consider an upper limit of 0.5 for the ECC.

$$\rho_{ecc_{ij}} = \left|\frac{|S_{ii}^{*}S_{ij}+S_{ji}^{*}S_{jj}|}{\left|\left(1-|S_{ii}|^2-|S_{ji}|^2\right)\left(1-|S_{jj}|^2-|S_{ij}|^2\right)\right|}\right|^2 \tag{9}$$

(vii) DG

The DG, which is calculated using Equation (3), is another significant factor for establishing the diversity effectiveness.

$$DG = 10 \times \sqrt{1-\rho_{ecc}^2} \tag{10}$$

ρ_{ecc} is the ECC.

3.2 Analysis of 2 x 1 Circular patch with DGS

In this section, we examine the parameters of a 2 x 1 circular patch antenna incorporating a Defected Ground Structure (DGS). Figure 5 illustrates the S parameters for the proposed MIMO antenna featuring DGS.

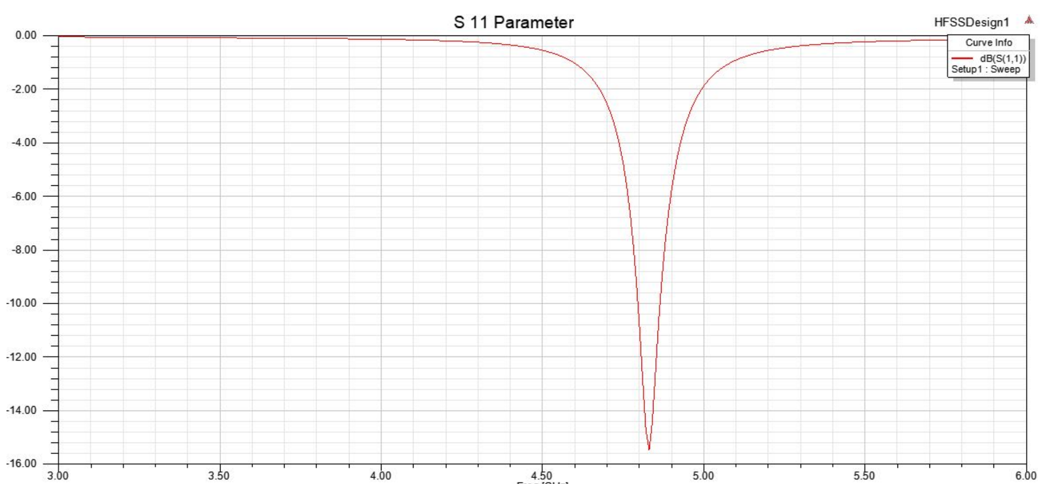

Figure 5. S parameter of the proposed MIMO antenna with DGS

The S parameters characterize the scattering behavior of the antenna and illustrate its response to external signals. The return loss (S11) quantifies the antenna's capacity to absorb energy from the source at its resonant frequency. For the 2x1 circular patch antenna with DGS, the measured return loss was -15.9 dB. This indicates that at the reverberating frequency of 4.83 GHz, the antenna effectively matched its input impedance to the transmission line. The return loss value reflects the antenna's resonance besides impedance matching capabilities by indicating the efficiency of power transfer beginning the cradle to the antenna. S21 and S12 denote the coupling between the two array elements, with lower values indicating improved isolation. The proposed antenna with DGS achieved an isolation parameter of -18 dB, as shown by S21 and S12. This value signifies that the two elements of the 2x1 array are effectively separated. A significant reduction in cross-coupling, evidenced by the -18 dB isolation, is essential in MIMO systems to mitigate interference between antennas. Figures 6 and 7 depict the isolation parameters for S12 and S21 with DGS, respectively.

Figure 6. S12 parameter of the proposed antenna with DGS

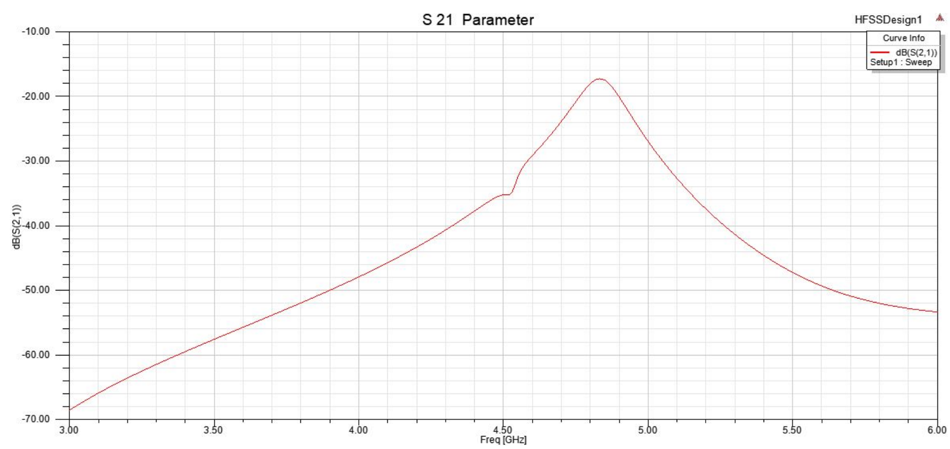

Figure 7. S21 parameter of the proposed antenna with DGS

The polar plot of improvement for the proposed 2 x 1 MIMO circular patch antenna is presented in Figure 8.

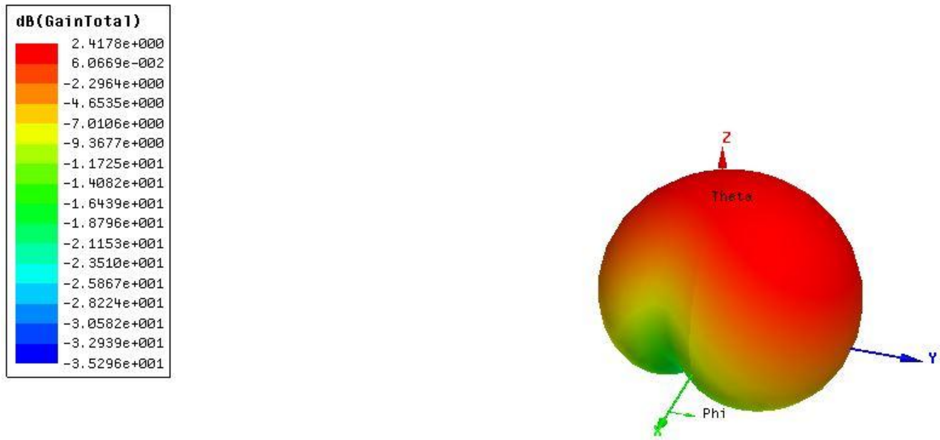

Figure 8. Gain of the proposed antenna with DGS

The polar gain plot indicated that the DGS antenna achieved a gain of 2.417 dB at its resonant frequency of 4.83 GHz. Antenna gain denotes to its capacity to emphasis and direct energy in a specific direction. The directivity of the proposed 2 x 1 circular patch antenna featuring DGS is illustrated in Figure 9.

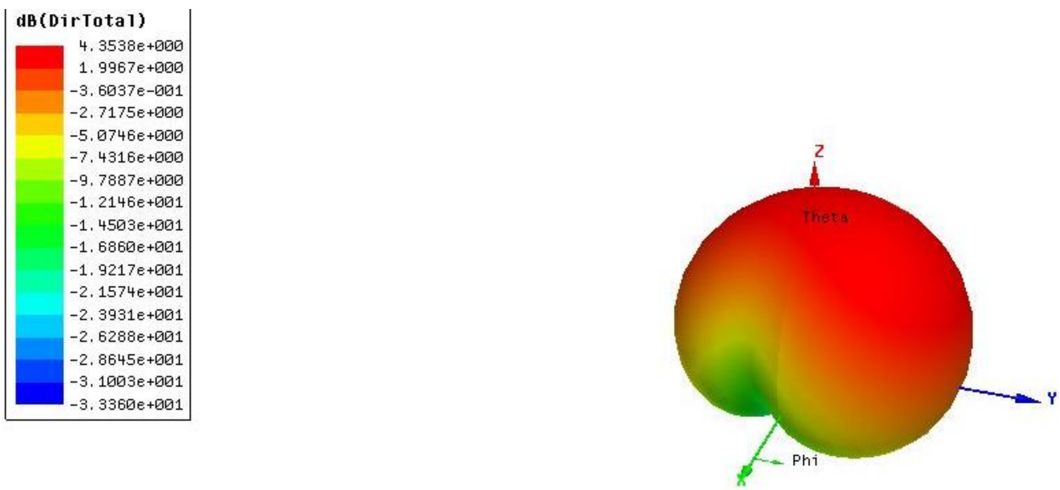

Figure 9. Directivity of the proposed antenna with DGS

The directivity of an antenna indicates the extent to which its radiation is concentrated in a specific direction. A higher directivity suggests that the antenna produces a more concentrated radiation pattern. Conversely, the antenna designed with DGS exhibits a directivity of 4.35 dB, indicating its high directivity. The ECC for this DGS-equipped antenna is illustrated in diagram 10.

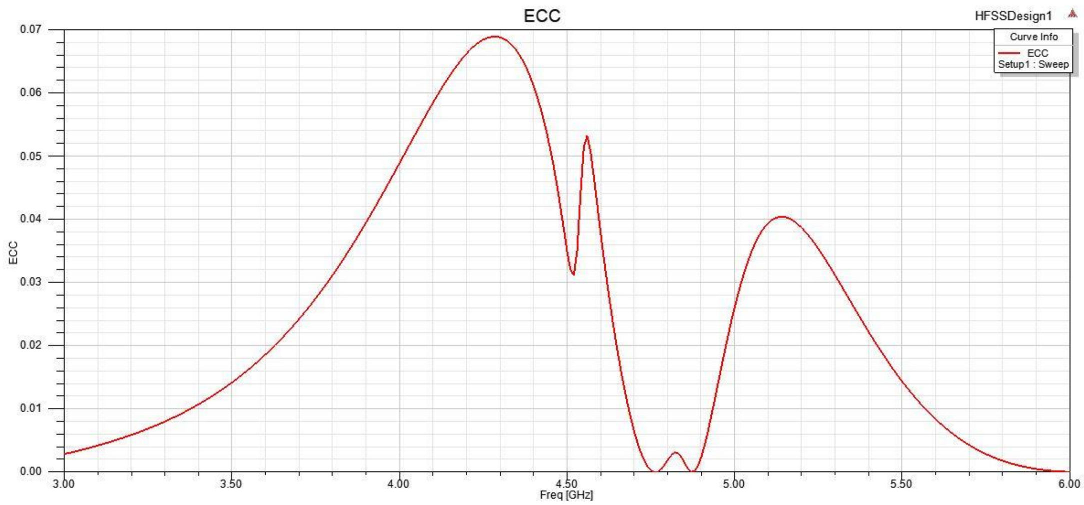

Figure 10. ECC of the proposed antenna with DGS

In MIMO systems, the Envelope Correlation Coefficient (ECC) is a critical metric. The ECC value for the antenna featuring a Defected Ground Structure (DGS) was recorded at less than 0.001, indicating minimal correlation between the two antenna elements. This low correlation suggests that the antennas are nearly orthogonal, allowing MIMO systems to effectively transmit and receive distinct signals simultaneously. The ECC serves as a measure of an antenna's efficiency in radiating energy in specific directions compared to an ideal radiator. The DGS's ECC result of under 0.001 reflects excellent performance. Figure 11 illustrates the proposed 2 x 1 circular patch antenna designed with DGS.

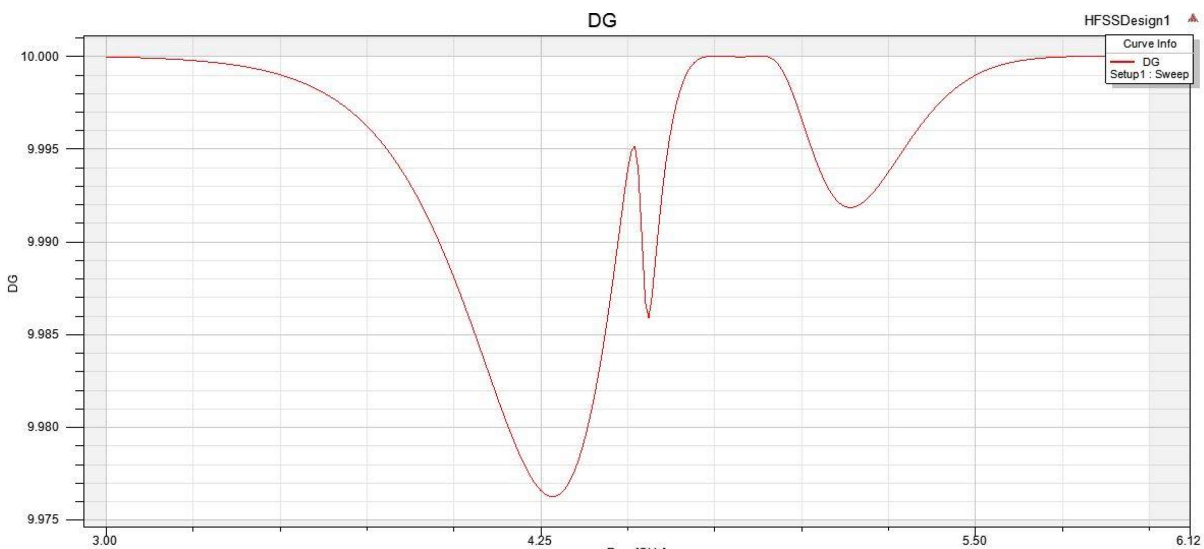

Figure 11. DG of the projected antenna with DGS

The suggested antenna demonstrated a Diversity Gain (DG) exceeding 10.00 when utilizing DGS at the resonant frequency of 4.83 GHz. Diversity gain refers to the enhancement in signal quality achieved through the use of multiple antennas within a system. A DG surpassing 10.00 serves as a reliable indicator of the antenna's ability to enhance signal reception quality across various conditions, thereby proving its utility in real-world applications.

3.3 Analysis of 2 x 1 Circular patch without DGS

In this section, the parameters of 2 x 1 circular patch antenna are analysed without DGS. The S parameter for the projected MIMO antenna without DGS is illustrated in figure 12.

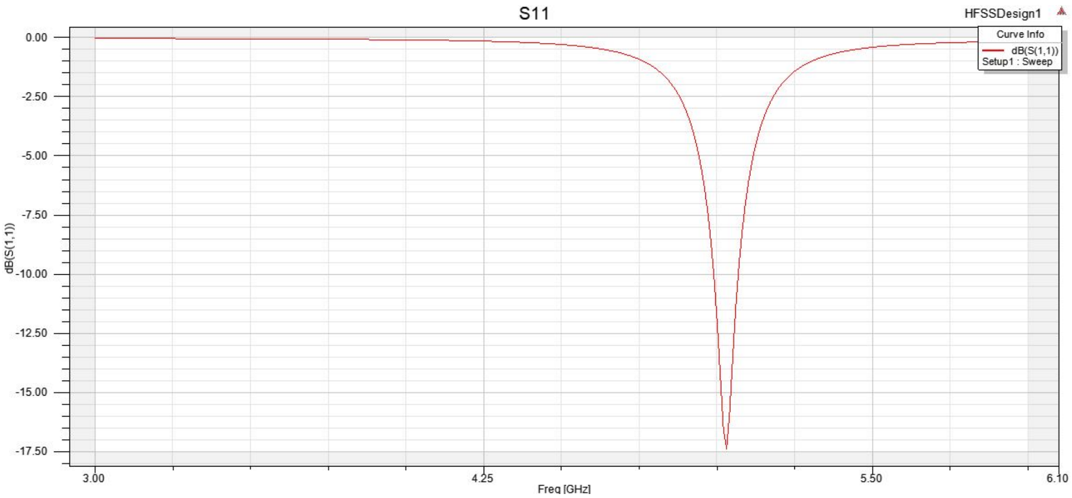

Figure 12. S parameters of the proposed MIMO antenna without DGS

At a frequency of 5.1 GHz, which is the resonance frequency, the reappearance loss of the antenna without DGS is measured at -17.49 dB. This designates that the antenna exhibits effective impedance matching and minimal reflected power at its resonant frequency. Isolation parameters for S21 and S12 without DGS are illustrated in Figures 13 and 14.

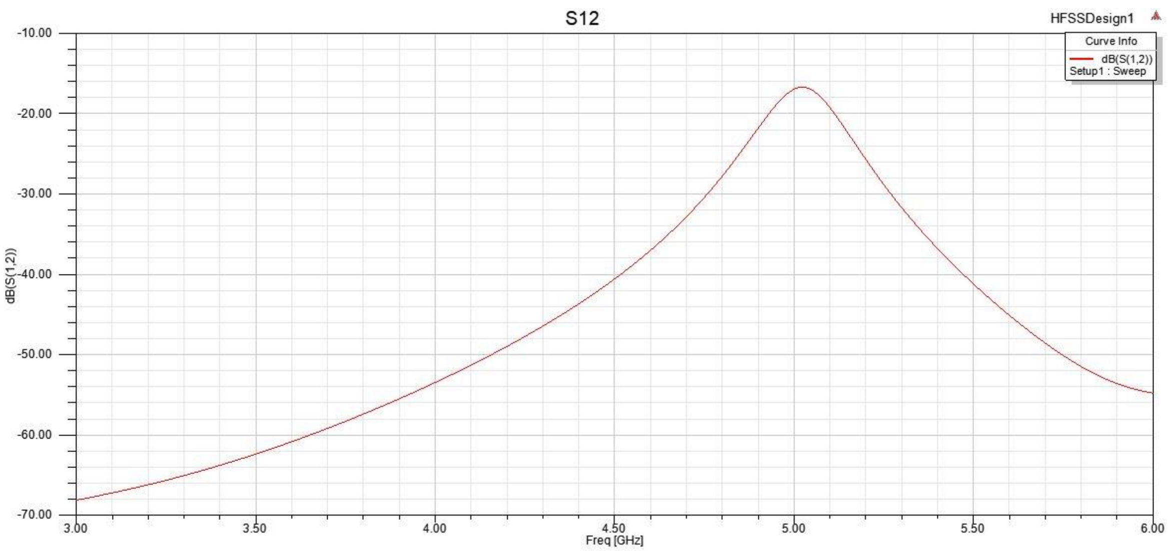

Figure 13. S12 parameter of the projected antenna without DGS

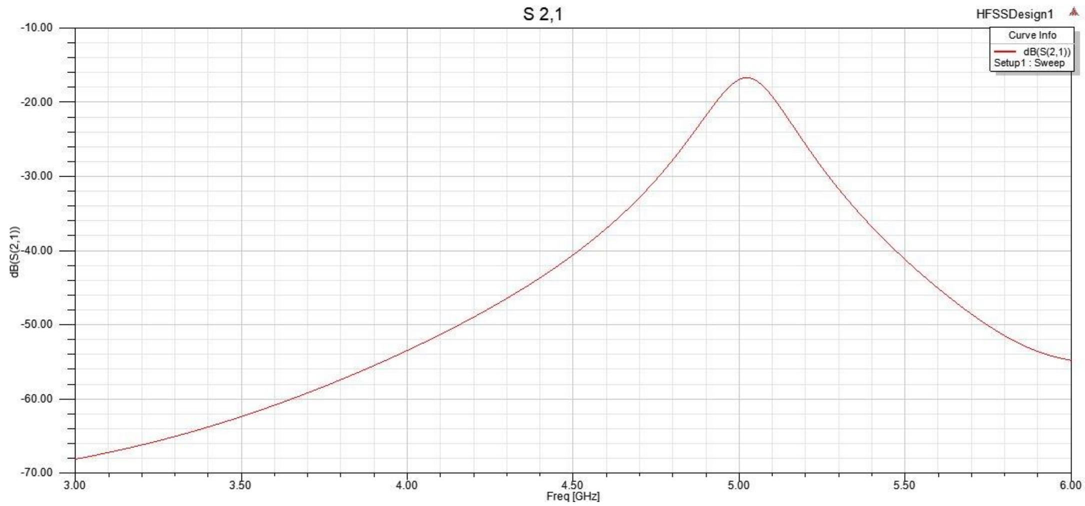

Figure 14. S21 parameter of the projected antenna without DGS

The isolation between the two antenna ports without DGS measures -18 dB, indicating minimal interaction between the antenna elements. Figure 15 illustrates the gain polar plot for the proposed 2 x 1 circular patch antenna without DGS.

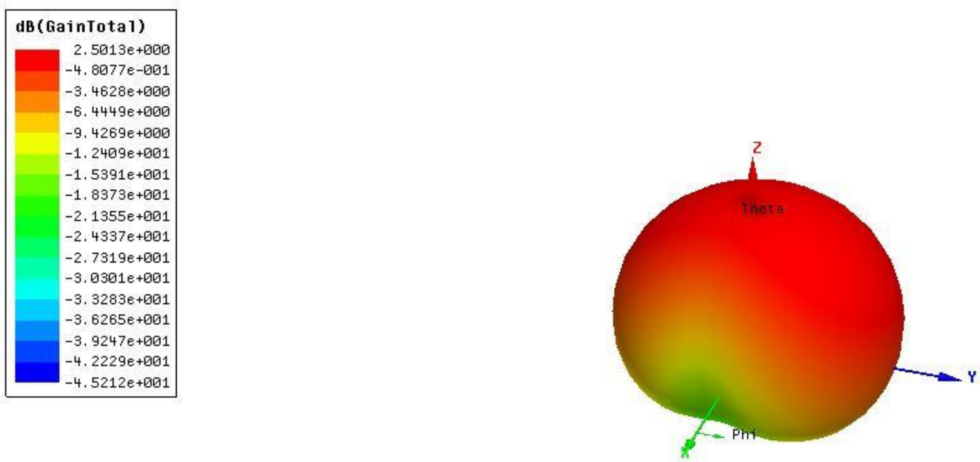

Figure 15. Gain of the projected antenna without DGS

The data indicates that the gain at the resonant frequency of 4.83, in the absence of DGS, is 2.50 dB. Additionally, Figure 16 illustrates the directivity of the proposed 2 x 1 circular patch antenna without DGS.

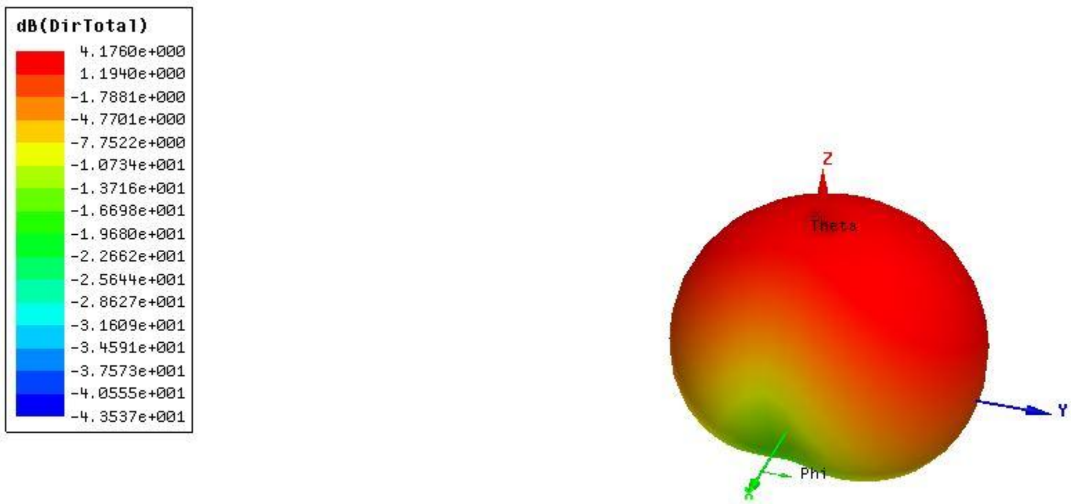

Figure 16. Directivity of the proposed antenna without DGS

The figure illustrates that the recommended antenna obtained 4.17 dB without DGS. Figure 17 illustrates the ECC for the projected antenna deprived of DGS.

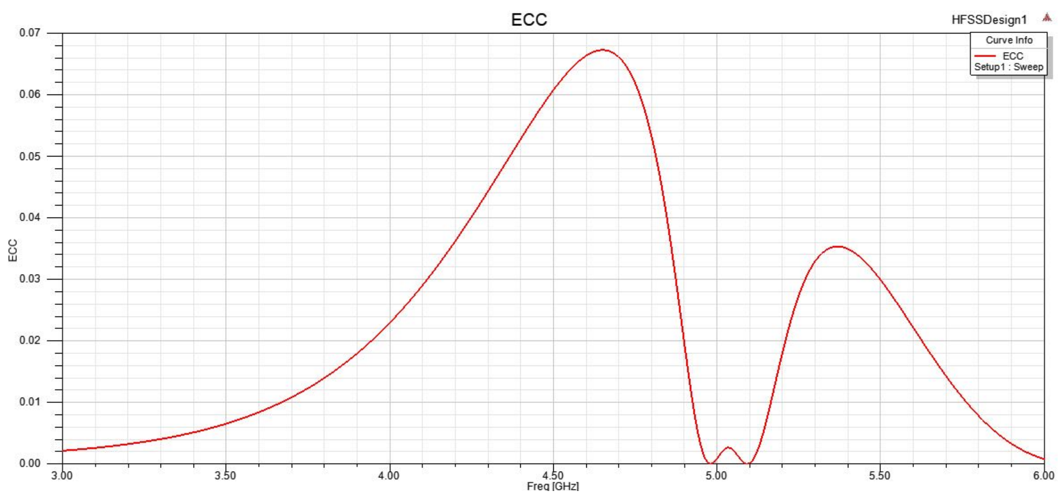

Figure 17. ECC of the projected antenna without DGS

The figure illustrates that without DGS, the suggested antenna attained a value of less than 0.001. Figure 18 shows the planned 2 x 1 circular patch antenna without DGS.

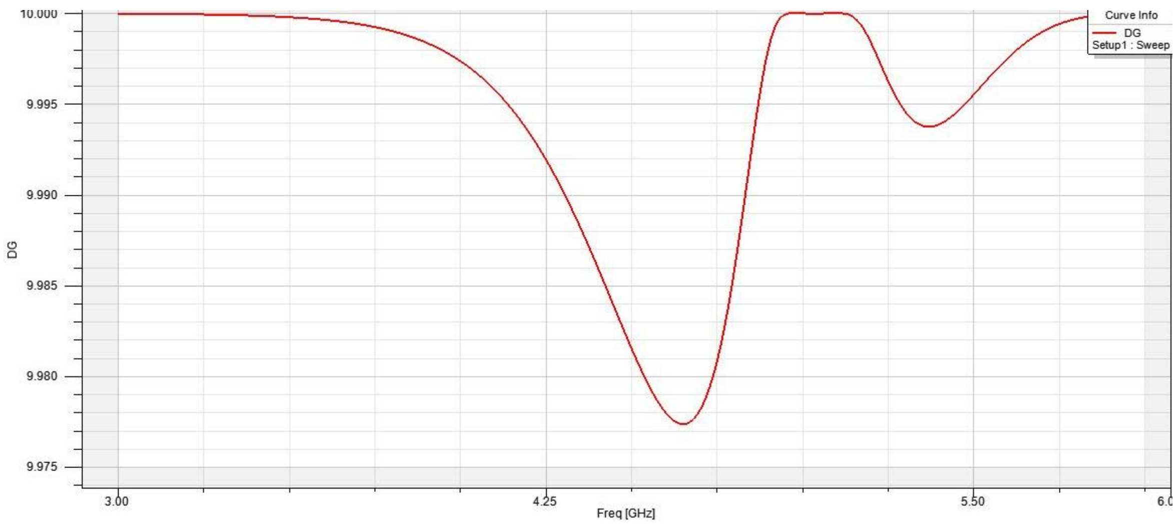

Figure 18. DG of the projected antenna without DGS

From the figure, it is observed that without the DGS the proposed antenna achieved the DG value of 10.00.

3.4 Comparison with the projected and prevailing method

Table 1 presents a assessment of the recital of the proposed MIMO 2 x 1 circular patch antenna against various existing literature, focusing on parameters including return loss, resonance frequency, substrate, gain, directivity, ECC, and DG.

Table 1. Comparison with the literature for the proposed and existing

Ref	**Substrate**	**Return loss (dB)**	**Isolation (dB)**	**Resonant frequency (GHz)**	**Gain (dB)**	**ECC**	**DG**	**Dir (dBi)**
16	FR4	-29	>20	2.4	-	<0.4	>9.8	-
19	FR4	12.07	33.4	4.1	-	<0.1	10	-
21	FR4	-23	<18	4.2	4	>0.01	>9.96	-
Proposed With DGS	FR4	-15.9	-18	4.83	2.41	<0.0001	>10	4.35
Without DGS	FR4	-17	-18	5	2.5	<0.001	10	4.17

The proposed MIMO antenna, both with and without DGS, demonstrated improved performance regarding directivity and isolation. Consequently, this antenna design is highly effective in enhancing isolation and minimizing mutual coupling.

4. Conclusion

This research study presents an innovative approach to enhancing the performance of a 2x1 MIMO circular microstrip patch antenna (MPA) tailored for Ultra-Wideband (UWB) solicitations. The integration of Defected Ground Structure (DGS) significantly enhances the electromagnetic characteristics of the antenna's ground plane by mitigating unwanted radiation modes and optimizing impedance matching. Detailed replications conducted spending High-Frequency Structure Simulator (HFSS) software indicate that the proposed MIMO antenna achieves a reappearance loss of -15.9 dB, a gain of 2.417 dB, and a directivity of 4.35 dB at a resonance frequency of 4.83 GHz, along with a Diversity Gain exceeding 10.00 dB. These outcomes underscore the efficacy of the projected design in addressing the cumulative ultimatum for high facts rates and superior signal quality in contemporary wireless communication systems.

References

1. Ghosh, S. and Sen, D., 2019. An inclusive survey on array antenna design for millimeter-wave communications. IEEE Access, 7, pp.83137-83161.
2. Wang, F., Duan, Z., Wang, X., Zhou, Q. and Gong, Y., 2019. High isolation millimeter-wave wideband MIMO antenna for 5G communication. International Journal of Antennas and Propagation, 2019.
3. Addepalli, T. and Anitha, V.R., 2021. Design and analysis of a novel compact spanner-shaped ultra-wideband antenna for MIMO systems. International Journal of Communication Systems, 34(5), p.e4739.
4. Ullah, U., Mabrouk, I.B., Koziel, S. and Al-Hasan, M., 2020. Implementation of spatial/polarization diversity for improved-performance circularly polarized multiple-input-multiple-output ultra-wideband antenna. IEEE Access, 8, pp.64112-64119.
5. Alsudani, A. and Marhoon, H.M., 2022. Performance enhancement of microstrip patch antenna based on frequency selective surface substrate for 5G communication applications. Evolution (N. Y), 4, p.7.
6. Srivastava, H., Singh, A., Rajeev, A. and Tiwari, U., 2020. Bandwidth and gain enhancement of rectangular microstrip patch antenna (RMPA) using slotted array technique. Wireless Personal Communications, 114, pp.699-709.
7. Babu, K.V. and Anuradha, B., 2019. Design of MIMO antenna to interference inherent for ultra wide band systems using defected ground structure. Microwave and Optical Technology Letters, 61(12), pp.2698-2708.
8. Babu, K.V. and Anuradha, B., 2021. Design of UWB MIMO antenna to reduce the mutual coupling using defected ground structure. Wireless Personal Communications, 118(4), pp.3469-3484.
9. Zaidi, A., Awan, W.A., Ghaffar, A., Alzaidi, M.S., Alsharef, M., Elkamchouchi, D.H., Ghoneim, S.S. and Alharbi, T.E., 2022. A low profile ultra-wideband antenna with reconfigurable notch band characteristics for smart electronic systems. Micromachines, 13(11), p.1803.
10. Ahmad, S., Khan, S., Manzoor, B., Soruri, M., Alibakhshikenari, M., Dalarsson, M. and Falcone, F., 2022. A compact CPW-fed ultra-wideband multi-input-multi-output (MIMO) antenna for wireless communication networks. IEEE Access, 10, pp.25278-25289.
11. Annou, A., Berhab, S. and Chebbara, F., 2020. Metamaterial-fractal-defected ground structure concepts combining for highly miniaturized triple-band antenna design. Journal of Microwaves, Optoelectronics and Electromagnetic Applications, 19, pp.522-541.
12. Rao, M.J., Satwika, B.V.S., Kowshik, D. and Srikavya, B., 2022. Simulation of Rectangular Microstrip Patch Antenna with Defected Ground Structure of H-Shape for C-Band Applications. International Journal of Research in Engineering, Science and Management, 5(6), pp.166-168.
13. Khalid, M., Iffat Naqvi, S., Hussain, N., Rahman, M., Fawad, Mirjavadi, S.S., Khan, M.J. and Amin, Y., 2020. 4-Port MIMO antenna with defected ground structure for 5G millimeter wave applications. Electronics, 9(1), p.71.
14. Desai, A., Bui, C.D., Patel, J., Upadhyaya, T., Byun, G. and Nguyen, T.K., 2020. Compact wideband four element optically transparent MIMO antenna for mm-wave 5G applications. Ieee Access, 8, pp.194206-194217.
15. Marotkar, D.S. and Zade, P., 2016, March. Bandwidth enhancement of microstrip patch antenna using defected ground structure. In 2016 International conference on electrical, electronics, and optimization techniques (ICEEOT) (pp. 1712-1716). IEEE.
16. Biswas, A.K. and Chakraborty, U., 2019. Reduced mutual coupling of compact MIMO antenna designed for WLAN and WiMAX applications. International Journal of RF and Microwave Computer-Aided Engineering, 29(3), p.e21629.
17. Zhang, Z., Kun, W.E.I., Jian, X.I.E., Jianying, L.I. and Ling, W.A.N.G., 2018. The MIMO Antenna Array with Mutual Coupling Reduction and Cross-polarization Suppression by Defected Ground Structures. Radioengineering, 27(4).
18. Hasan, M.N., Chu, S. and Bashir, S., 2019. A DGS monopole antenna loaded with U-shape stub for UWB MIMO applications. Microwave and optical technology letters, 61(9), pp.2141-2149.
19. Shiddanagouda, F.B., RM, V. and Hunagund, P.V., 2020. A Microstrip-Line Fed Quad-Port MIMO Antenna with Defected Ground Structures for Wireless Applications. International Journal of Advances in Microwave Technology, 5(1), pp.218-222.
20. Nguyen, N.L., 2019. Gain enhancement in MIMO antennas using defected ground structure. Progress In Electromagnetics Research M, 87, pp.127-136.
21. Khan, M.K., Feng, Q. and Zheng, Z., 2021. Experimental investigation and design of UWB MIMO antenna with enhanced isolation. Progress In Electromagnetics Research C, 107, pp.287-297.
22. Teja, M.S. and Rao, P.S., 2017. Isolation enhancement of a very compact uwb-mimo slot antenna with two defected ground structures used in multi band applications. International Research Journal of Engineering and Technology (IRJET), 4, pp.1967-1971.
23. Tang, X., Yao, Z., Li, Y., Zong, W., Liu, G. and Shan, F., 2021. A high performance UWB MIMO antenna with defected ground structure and U-shape branches. International Journal of RF and Microwave Computer-Aided Engineering, 31(2), p.e22270.

24. Islam, M.S., Ibrahimy, M.I., Motakabber, S.M.A., Hossain, A.Z. and Azam, S.K., 2019. Microstrip patch antenna with defected ground structure for biomedical application. Bulletin of Electrical Engineering and Informatics, 8(2), pp.586-595.
25. Nawale, P.A. and Zope, R.G., 2014. Design and Improvement of microstrip patch antenna parameters using defected ground structure. Diamond, 13, pp.20-89.
26. Sohi, A.K. and Kaur, A., 2020. UWB aperture coupled circular fractal MIMO antenna with a complementary rectangular spiral defected ground structure (DGS) for 4G/WLAN/radar/satellite/international space station (ISS) communication systems. Journal of Electromagnetic waves and Applications, 34(17), pp.2317-2338.
27. Sohi, A.K. and Kaur, A., 2021. Triple band-stop characteristics from an aperture coupled modified Pythagorean tree fractal-based UWB-MIMO antenna integrated with complementary hexagonal spiral defected ground structure. AEU-International Journal of Electronics and Communications, 137, p.153805.
28. Jamal, M.Y., Li, M. and Yeung, K.L., 2020. Isolation enhancement of closely packed dual circularly polarized MIMO antenna using hybrid technique. IEEE Access, 8, pp.11241-11247.
29. Babu, K.V. and Anuradha, B., 2019. Design and analysis of multi-band circle shape MIMO antenna using defected ground structure to reduce mutual coupling. International Journal of Ultra Wideband Communications and Systems, 4(1), pp.32-40.
30. Babu, K.V. and Anuradha, B., 2019. Design of MIMO antenna to interference inherent for ultra wide band systems using defected ground structure. Microwave and Optical Technology Letters, 61(12), pp.2698-2708.
31. Khandelwal, M.K., Kanaujia, B.K. and Kumar, S., 2017. Defected ground structure: fundamentals, analysis, and applications in modern wireless trends. International Journal of Antennas and Propagation, 2017.
32. Kim, C.S., Park, J.S., Ahn, D. and Lim, J.B., 2000. A novel 1-D periodic defected ground structure for planar circuits. IEEE Microwave and Guided Wave Letters, 10(4), pp.131-133.
33. Acharjee, J., Mandal, K., Mandal, S.K. and Sarkar, P.P., 2016, January. Mutual coupling reduction between microstrip patch antennas by using a string of H-shaped DGS. In 2016 International Conference on Microelectronics, Computing and Communications (MicroCom) (pp. 1-3). IEEE.